Characterization of roll bite heat transfers in hot steel strip rolling and their influence on roll thermal fatigue degradation

Nicolas Legrand, Daniel Weisz-Patrault, Jaroslav Horsky, Tomas Luks, Nathalie Labbe, Michel Picard, Alain Ehrlacher

Characterization of roll bite heat transfers in hot steel strip rolling and their influence on roll thermal fatigue degradation

N. Legrand[1,a], D. Weisz-Patrault[2,b],

J. Horsky[3,g], T. Luks[3,f], N. Labbe [1,c] M. Picard[1,d], A. Ehrlacher[2,e]

[1]ArcelorMittal Maizières Research, Maizieres-les-Metz, France

[2]Université Paris-Est, U.R. Navier, Ecole des Ponts et Chaussées, Marne la Vallée, France

[3]Brno University of Technology, Brno, Czech republic

[a]nicolas.legrand@arcelormittal.com, [b]daniel.patrault@enpc.fr, [c]nathalie.labbe@arcelormittal.com, [d]michel.picard@arcelormittal.com, [e]alain.ehrlacher@enpc.fr, [f]luks@LPTaP.fme.vutbr.cz, [g]horsky@fme.vutbr.cz

Keywords: hot strip rolling, steel, roll bite heat transfer, inverse thermal analysis, thermal fatigue

Abstract.

A temperature sensor with a thermocouple placed at ~0.5 mm from roll surface is used in hot rolling conditions to evaluate by inverse calculation heat transfers in the roll bite. Simulation analysis under industrial hot rolling conditions with short contact lengths (e.g. short contact times) and high rolling speeds (7 m./sec.) show that the temperature sensor + inverse analysis with a high acquisition frequency (> 1000 Hz) is capable to predict accurately (5 to 10% error) the roll bite peak of temperature as well as the roll surface temperature evolution all around the roll rotation. However as heat flux is more sensitive to noise measurement, the peak of heat flux in the bite is under-estimated (20% error) by the inverse calculation and thus the average roll bite heat flux is also interesting information from the sensor (these simulation results will be verified with an industrial trial that is being prepared).

Rolling tests on a pilot mill with low rolling speeds (from 0.3 to 1.5 m./sec.) and strip reductions varying from 10 to 40% have been performed with the temperature sensor. Analysis of the tests by inverse calculation show that at low speed (<0.5 m./sec.) and large contact lengths (reduction: 30 to 40%), the roll bite peak of heat flux reconstructed by inverse calculation is correct. At higher speeds (1.5 m./sec.) and smaller contact lengths (reduction : 10-20%), the reconstruction is incorrect: heat flux peak in the bite is under-estimated by the inverse calculation though its average value is correct.

The analysis reveals also that the Heat Transfer Coefficient $HTC_{roll\text{-}bite}$ (characterizing heat transfers between roll and strip in the bite) is not uniform along the roll bite but is proportional to the local rolling pressure.

Finally, based on the above results, simulations with a roll thermal fatigue degradation model under industrial hot rolling conditions show that the non-uniform roll bite Heat Transfer Coefficient $HTC_{roll\text{-}bite}$ may have under certain rolling conditions a stronger influence on roll thermal fatigue degradation than the equivalent (e.g. same average) $HTC_{roll\text{-}bite}$ taken uniform along the bite. Consequently, to be realistic the roll thermal fatigue degradation model has to incorporate this non-uniform $HTC_{roll\text{-}bite}$.

1. INTRODUCTION

In hot rolling, thermal solicitations of rolls are characterized by cyclic thermal shocks in the roll bite due to the cyclic contact between a strip at ~1000°C and a roll at 50-100°C. This cyclic thermal loading, amplified with work roll water cooling, is responsible for roll degradation by thermal fatigue that strongly shorten rolls life. A decrease of roll thermal fatigue requires a better knowledge of real peaks of temperature and heat transfers in the roll bite that are the source of the roll thermal shock. Currently, these roll bite peaks are approximated with Heat Transfer Coefficients 'HTC' macroscopically tuned on measured mill data. This current way of identification is sufficient to optimize mill cooling capacity where only a knowledge of the average heat transfer within and from the roll is needed. However, to determine roll degradation by thermal fatigue, an accurate and local evaluation of these roll bite peaks of temperature and heat flux is necessary. This paper determines the specifications of a temperature sensor to evaluate these peaks under hot rolling conditions. It also shows how heat transfers and temperatures distributions along the roll bite affect roll thermal fatigue.

2. HEAT TRANSFER MODELS

Two different heat transfer models are used to analyze roll temperature sensors measurements: ***- model n°1:*** a 2D semi-analytical temperature evolution model [2-3] (computation time for one roll revolution ~0.05 s.) is used in inverse mode: temperature measured with sensors at inner roll radius is used to predict (reconstruct) *roll surface heat flux* and *temperature*. The 2D unsteady heat equation is solved for the roll (T: temperature, t: time, r,θ: roll positions, ω: rotation speed, D: thermal diffusivity):

$$\frac{\partial^2 T}{\partial r^2} + \frac{1}{r}.\frac{\partial T}{\partial r} + \frac{1}{r^2}.\frac{\partial^2 T}{\partial \theta^2} = \frac{1}{D}\left(\frac{\partial T}{\partial t} + \omega \frac{\partial T}{\partial \theta}\right) \quad (1)$$

As the model is analytical, it considers thermal properties independent of temperature: λ (thermal conductivity) = 17.3 W/m/K and D (thermal diffusivity) = 4.2 mm^2/sec. These values, determined by calibration, correspond to average thermal properties of solder material used in the slot sensor.

- model n°2: a numerical finite difference roll gap heat transfer model for the strip coupled with a finite difference 1D roll temperature evolution model [4] is used in direct mode: the roll-bite Heat Transfer Coefficient $HTC_{roll\text{-}bite}$, thermal boundary condition of the model, is adjusted to match simultaneously sub-surface temperatures and roll surface and heat flux obtained respectively by the temperature sensor and by model n°1. The following 1D heat equation is solved for the roll:

$$\frac{\partial^2 T}{\partial r^2} + \frac{1}{r}.\frac{\partial T}{\partial r} = \frac{1}{D}\left(\frac{\partial T}{\partial t}\right) \quad (2)$$

The model can consider heat dissipation by friction in the bite and roll thermal properties dependent on temperature: λ varies from 44 to 35 W/m/K and D varies from 11 to 6.5 mm^2/sec. for temperature varying from 20 to 550°C. These values correspond to thermal properties of a normal steel grade which is the grade used for the work rolls. Model n°2 cannot consider the sensor in the work roll, however as shown further in the paper, the solder material (Ni based material) of the sensor can be considered in model n°2 through a roll surface coating of 0.65 mm thickness.

3. DESIGN OF THE TEMPERATURE SENSOR AND DATA ACQUISITION SYSTEM *(simulation analysis)*

An industrial hot rolling condition has been considered in the following simulation analysis: last roll revolution after 56 coils rolling on the 4th stand of a 6-stands finishing mill has been used for the

following calculations: entry/exit thickness: 5.15/3.35 mm, roll speed = 7 m./sec., entry strip temperature: 896°C, roll water cooling applied at entry and exit of the stand.

Determination of the maximum distance of sensor to roll surface:

There is a maximum distance of the thermocouple to roll surface that enables by inverse analysis (model n°1) a correct evaluation of roll bite peak of temperature and peak of heat flux. This distance depends on the thermal skin thickness, e.g. the thickness near roll surface where temperature varies significantly at each roll rotation: the sensor must be placed in this zone otherwise if it is located further, the sub-surface temperature signal obtained with the sensor is too low to allow correct reconstruction. A numerical application of this thermal skin thickness gives 0.7 mm for the above industrial hot rolling conditions: Roll thermal skin thickness: $\delta = \sqrt{\frac{2.a}{\omega}}$ (a: roll thermal diffusivity ~ 5 mm^2/sec., ω: roll rotation speed = 7 m./sec. = 30 rad./sec). The distance depends also (but to a lesser extent) on noise level.

In the next section, this distance has been determined by direct/inverse calculations: in a first step, a sub-surface measurement is simulated at three different distances (0.48 mm, 0.8 mm, 1.2 mm) by direct calculations using model n°2 with a known surface heat flux and temperature. Then white noise with +/-1°K amplitude is introduced in these simulated sub-surface measurements to evaluate noise influence. In a second step, inverse calculations (model n°1) are made using these simulated measurements to recalculate the surface heat flux and temperature.

The quality of reconstruction of temperature and heat flux at roll surface is evaluated by comparison of heat flux and temperature obtained from model n°1 and from model n°2. Results presented on fig. 1 show that with white noise measurement, the maximum thermocouple depth under the surface to obtain a good reconstruction is ~0.5 mm. A longer distance (0.8 and 1.2 mm) under-estimates the roll bite peak of temperature by 13 and 26% respectively, which is in accordance with the roll thermal skin thickness value estimation (0.7 mm: see above).

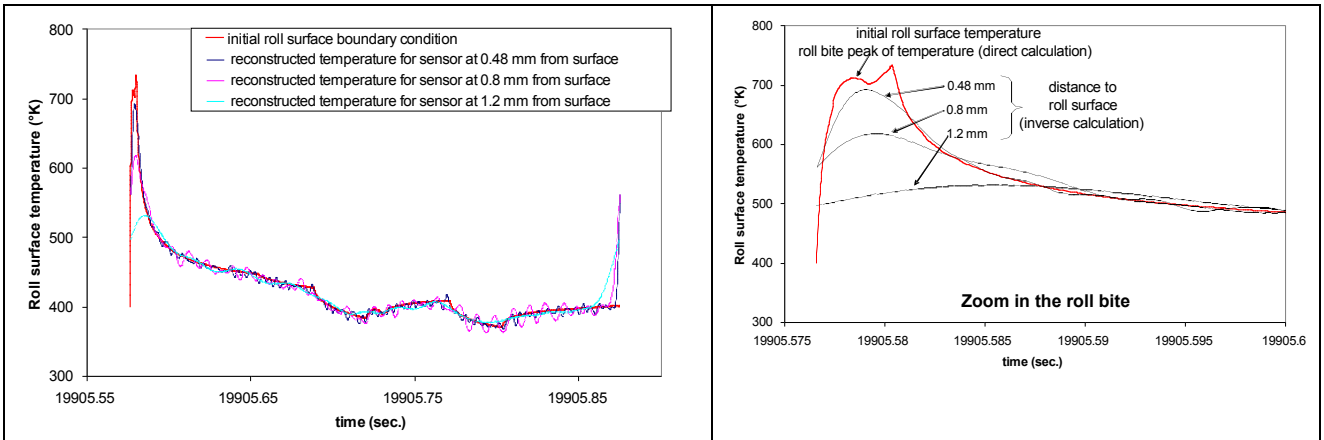

a) roll surface temperature evolution

b) roll surface temperature evolution: zoom in the bite

Fig. 1: Evaluation by direct/inverse simulation of reconstructed surface temperature for 3 different distances of temperature sensor to roll surface: 0.48 – 0.8 – 1.2 mm.

Determination of the optimum acquisition frequency for measurement of sub-surface temperature:

Using the same methodology and 0.48 mm for the distance of temperature sensor to roll surface, the optimum frequency for the temperature to obtain a correct reconstruction of the peak of temperature and peak of heat flux at roll surface in the roll bite is determined. Three acquisition frequencies (300, 1000, 3000 Hz) are considered for the simulated sub-surface measured temperature by down-sampling a temperature calculated with a very small time step to generate a quasi-continuous sub-surface temperature signal. In fig. 2 the reconstructed surface temperature profile (model n°1) is presented (for inputs at three acquisition frequencies) and compared to the simulated temperature

profile (model n°2). Frequency of acquisition seems not to be a significant issue for the reconstruction accuracy. Results show that the temperature is reconstructed properly (error less than 10%: fig.3-a) with very limiting oscillations.

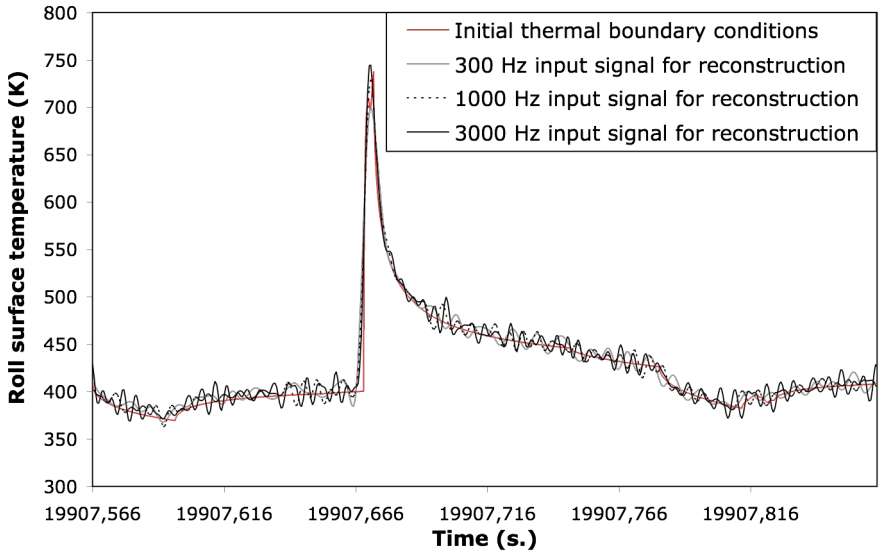

Fig. 2: evaluation by direct/inverse simulations of reconstructed roll surface temperature for 3 different acquisition frequencies for the sub-surface temperature at a distance of 0.48 mm – last roll rotation of coil n°56

Fig.3-a and 3-b are zooms in the bite of temperature and heat flux reconstructions: an acquisition frequency of 1000 or 3000 Hz is better for the reconstruction of surface heat flux. However, the peak of heat flux is under-estimated by 20% (fig. 3-b).

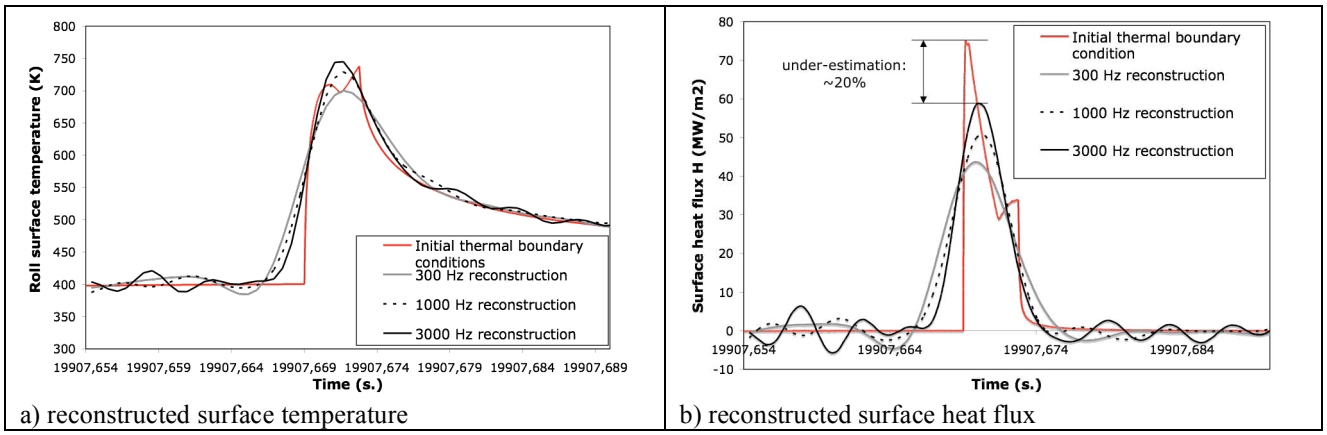

a) reconstructed surface temperature

b) reconstructed surface heat flux

Fig. 3: zoom in the roll bite area (last roll rotation of coil n°56: Evaluation by direct/inverse simulation of reconstructed roll surface temperature and reconstructed heat flux for 3 acquisition frequencies for the sub-surface temperature (distance: 0.48 mm)

This lower quality of reconstruction of the surface heat flux compared with the surface temperature is due to the noise introduced in the simulation on the input temperature signal[1]: as surface heat flux is obtained from temperature gradient (derived signal), it is more sensitive than temperature to noise and so its reconstruction to roll surface is more difficult. Nevertheless, it has been verified that average heat flux is correctly evaluated by inverse calculation even if the local heat flux peak is not perfectly evaluated: heat flux integrated over the enlarged roll bite area gives the average real roll bite heat flux introduced in the direct calculation, which is valuable information. As a conclusion of

[1] this white noise is difficult to filter as it affects all frequencies

these simulation results, an optimum acquisition frequency is considered to be within 1000-3000 Hz: it enables a correct evaluation of temperature peak and rather correct heat flux peak in the roll.

4. HOT PILOT MILL TRIALS

Roll temperature sensors (fig.4)

Roll temperature sensors are manufactured with a K-type thermocouple (diameter = 0.5 mm) implemented in a cylindrical plug. The work roll is drilled with one axial hole and 4 radial holes, then the plugs with a slightly higher dimension than the holes (dimension difference: 1‰) are inserted into the different radial holes with a press (fig. 4a). The surface of the roll is finally re-reground in order to have a smoothed roll surface. The thermocouple wire is parallel to roll surface (not perpendicular) to avoid perturbations of isotherms.

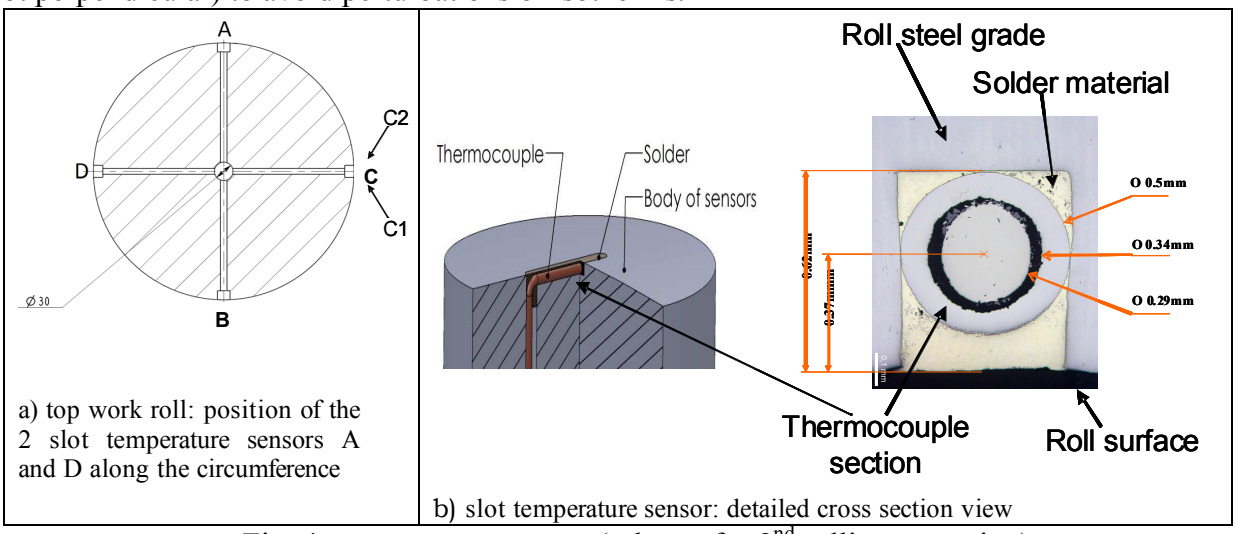

a) top work roll: position of the 2 slot temperature sensors A and D along the circumference

b) slot temperature sensor: detailed cross section view

Fig. 4: temperature sensors (scheme for 2nd rolling campaign)

Based on results from **[5]**, a slot type temperature sensor has been used in this study (fig.4b): the thermocouple is placed in a slot made by milling at the surface of the plug and brazed to the rest of the plug. A Nickel based solder material covers the thermocouple. This sensor has a relatively fast response time **[5]**.

Sensors calibration

In accordance with the previous simulations, the thermocouple is placed at ~0.5 mm from roll surface. A calibration test with hot water (water temperature = 60 to 80°C) is performed to identify precisely this distance using a model of the sensor including thermal properties of the equivalent material surrounding the sensor (see details in **[2]**): the distance obtained is 0.51 mm for the first rolling campaign (test n°4) and 0.40 mm for the second rolling campaign (tests n°5 to 17) (table 1).

Pilot mill trials conditions

Aluminium killed grade strips (initial width/thickness = 100mm/60mm) were rolled on a hot pilot mill in 2-high configuration with the top work roll equipped with slot temperature sensors (work roll radius = 234.5 mm for first campaign and 232.5 mm for second campaign). In agreement with previous simulation results, temperature signals during rolling have been stored using a 3.6 kHz data acquisition system. The roll was cooled by air outside the roll bite (no water cooling) and heated by the strip inside the roll bite. These conditions have the advantage that heat transfer with air outside the bite is relatively well known and relatively constant along the roll circumference (HTC_{air} = 50 W/m^2/K), only $HTC_{roll\text{-}bite}$ is unknown. In comparison, industrial rolling conditions are more difficult to analyze because cooling by water is not known accurately and is added to the other unknown $HTC_{roll\text{-}bite}$.

Pilot mill trials results

Test results are reported in table 1: test n°4 combined with simulations enables to evaluate accurately the thermal response of the bi-material temperature sensor (thermocouple embedded in Ni surrounded by steel), tests n°5, 6, 8, 10 evaluate the strip reduction influence (10% to 40%), tests n°10, 11, 12, 13 and tests n°14, 15 evaluate the rolling speed influence respectively at high reduction (40%) and low reduction (10%), tests n°16 and 17 evaluate the scale thickness influence formed at strip surface before rolling. In the next section, for all the tests the slot temperature sensor SL-S has been used.

Table 1: Pilot hot rolling test results

		measured values							
test n°	**reduction per pass (target) (%)**	reduction per pass (real) (%)	**contact length** using real pass red. **(°)**	roll force (kN)	roll speed (m/sec.)	heating furnace temperature (°C)	time between furnace and rolling start (sec.)	strip temperature pyrometer 1 (°C)	strip temperature pyrometer 2 (°C)
4 (first campaign)	**20**	pass 1: 19.28 pass 2: 20.17 pass 3: 17.45 pass 4: 19.09	**12**	pass 1: 429 pass 2: 525 pass 3: 631 pass 4: 592	1.5	1150	0	pass 1: 1083 pass 2: 995 pass 3: 965 pass 4: 930	pass 1: 1000 pass 2: 987 pass 3: 927 pass 4: 920
5 (2nd campaign)	**10**	pass 1: 7.45 pass 2: 9.75	**8.4**	pass 1: 346 pass 2: 392	1.5	1050	0	pass 1: 1029 pass 2: 977	pass 1: 991 pass 2: 990
6 (2nd campaign)	**20**	pass 1: 16.61 pass 2: 19.34	**12**	pass 1: 610 pass 2: 672	1.5	1050	0	pass 1: 1029 pass 2: 977	pass 1: 918 pass 2: 932
8 (2nd campaign)	**30**	pass 1: 25.9 pass 2: 28.45	**14**	pass 1: 875 pass 2: 967	1.5	1050	0	pass 1: 1032 pass 2: 967	pass 1: 966 pass 2: 994
10 (2nd campaign)	**40**	pass 1: 35.1	**17.4**	pass 1: 1150	0.73	1050	0	pass 1: 1050	pass 1: 970
11 (2nd campaign)	**40**	pass 1: 35.4	**17.4**	pass 1: 1162	**0.35**	1050	0	pass 1: 1025	pass 1: 873
12 (2nd campaign)	**40**	pass 1: 35.8	**17.4**	pass 1: 1000	0.77	1050	0	pass 1: 1008	pass 1: 838
13 (2nd campaign)	**40**	pass 1: 35.5	**17.4**	pass 1: 1000 pass 2: 1300	0.41	1050	0	pass 1: 1011 pass 2: 932	pass 1: 860 pass 2: 862
14 (2nd campaign)	**10**	pass 1: 8 pass 2: 9.8	**8.4**	pass 1: 361 pass 2: 395	1.5	1050	0	pass 1: 1022 pass 2: 980	pass 1: 987 pass 2: 907
15 (2nd campaign)	**10**	pass 1: 8.5 pass 2: 9.7	**8.4**	pass 1: 323 pass 2: 380	**0.5**	1050	0	pass 1: 1030 pass 2: 983	pass 1: 964 pass 2: 1000
16 (2nd campaign)	**10**	pass 1: 8.15 pass 2: 9.6	**8.4**	pass 1: 404 pass 2: 475	1.5	1050	**60**	pass 1: 952 pass 2: 930	pass 1: 896 pass 2: /
17 (2nd campaign)	**10**	pass 1: 8.2 pass 2: 9.6	**8.4**	pass 1: 422 pass 2: 494	1.5	1050	0	pass 1: 983 pass 2: 907	pass 1: 914 pass 2: /

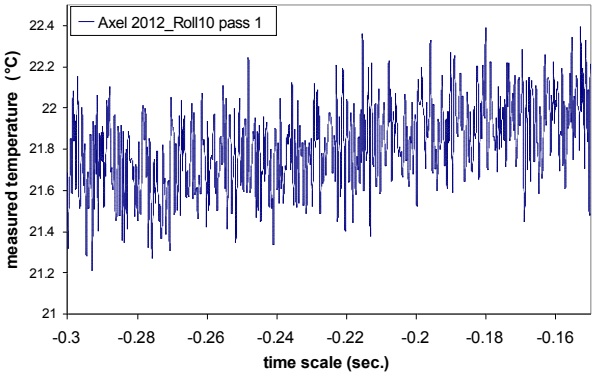

Fig.5: temperature signal for test n°10

Fig. 5 shows that the typical noise level on measured temperature signal is ~ +/- 0.5°C, which is a bit lower (though of same order) than the +/-1°C noise level used in simulations of section 3 of this paper.

Evaluation of roll surface temperature and roll surface heat flux by inverse calculation *(model n°1)*

Fig.5 shows for test n°6 the measured sub-surface and reconstructed surface temperatures obtained with the thermal inverse analysis (model n°1) over the three roll rotations of the first pass.

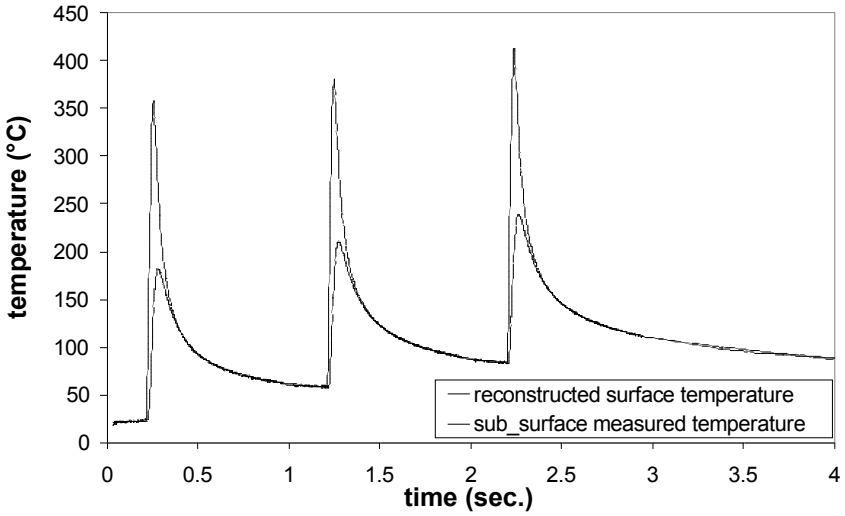

Fig.5: tests n°6 - 1st pass: 3 first roll revolutions: sub-surface measured and reconstructed surface temperatures

Sub-surface and surface temperatures are different only in the area of the roll bite (one quarter of roll rotation); the two temperatures become equal when roll surface is sufficiently far from the roll bite. Fig.6 shows a zoom of the first revolution of fig. 5. Radial and circumferential surface heat fluxes calculated by the 2D inverse analysis (model n°1) have also been added to that figure: even if the circumferential heat flux is much lower than the radial heat flux, it is a bit higher in the roll bite than over the rest of the roll rotation. This flux has also an opposite direction before and after the roll bite peak of temperature.

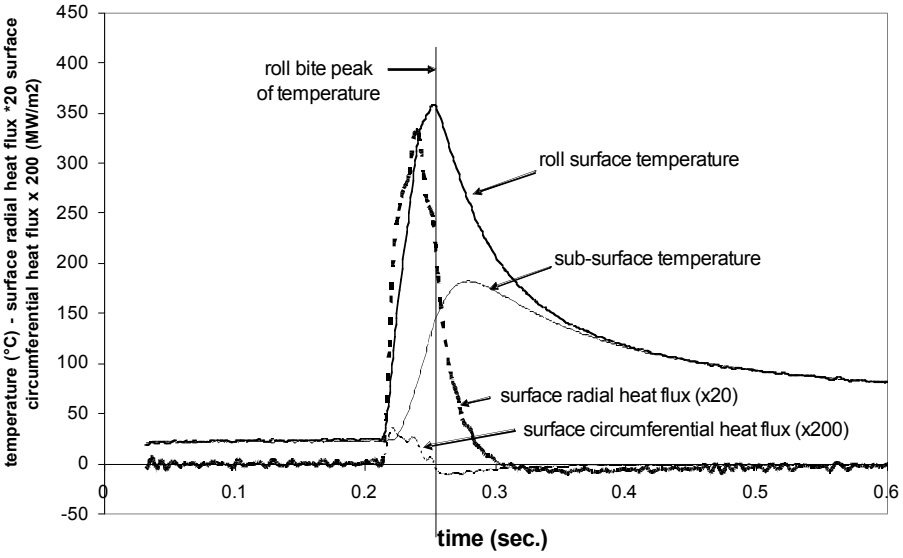

Fig.6: zoom on 1st revolution (test n°6) – measured temperature and recalculated surface heat flux, circumferential and radial heat fluxes

Strip reduction influence on heat transfers

Fig. 7 shows for different strip reductions (10%, 20%, 30%, 40%), the roll temperature measured at sub-surface during rolling (1st pass, 1st roll revolution for each test) and the reconstructed roll surface heat flux and roll surface temperature determined by inverse calculation with model n°1. However, the measured temperature and reconstructed heat flux and temperature at roll surface seem incorrect for the 30% reduction test, as shown by the negative heat flux for that test (fig. 7-c), thus this test will not be considered in the following analysis.

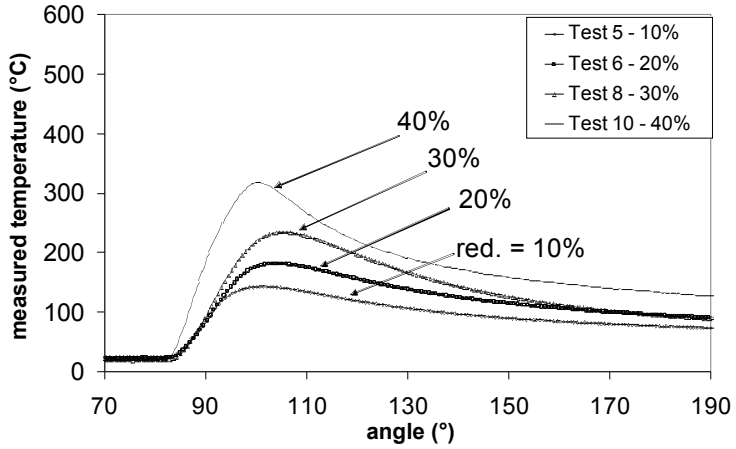

a) measured temperature at sub-surface

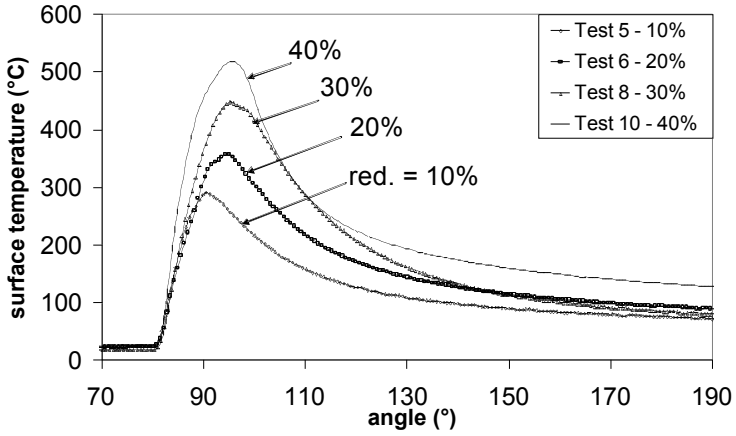

b) reconstructed temperature at roll surface

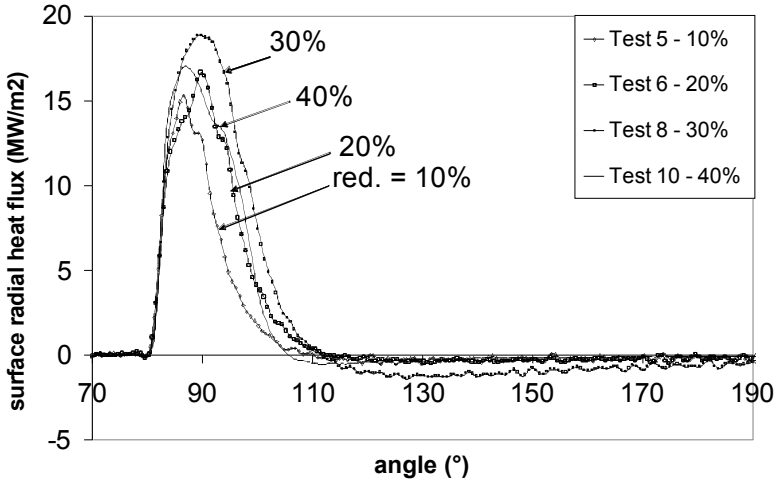

c) reconstructed heat flux at roll surface

Fig.7: strip reduction influence on heat transfers – tests n°5, 6, 8, 10: 1st pass – 1st revolution.

Compared to tests results obtained in the previous rolling campaign **[5]**, here reductions are higher (30%-40%) and so produce higher surface temperatures (450-500°C) and heat fluxes (17-18 MW/m^2) because $HTC_{roll\text{-}bite}$ is higher. These test results will be used in the next section to analyse the distribution of $HTC_{roll\text{-}bite}$.

Rolling speed influence on heat transfer

Fig.8 shows for 10% strip reduction the influence of two different rolling speeds on measured temperature and reconstructed temperature and heat flux at roll surface: a lower speed gives a longer roll-strip contact time so a higher heating time from strip to roll: this gives a much higher roll surface temperature. Fig.8-a shows also that the roll bite thermal contact length (length over which heat flux from the roll bite penetrates the roll) is two to three times larger than the direct (e.g. geometrical) roll-strip contact length (see table n°1). At lower speed, the thermal contact length of the heat flux is in better agreement with the geometrical roll bite size (fig. 8-b) than at higher speed.

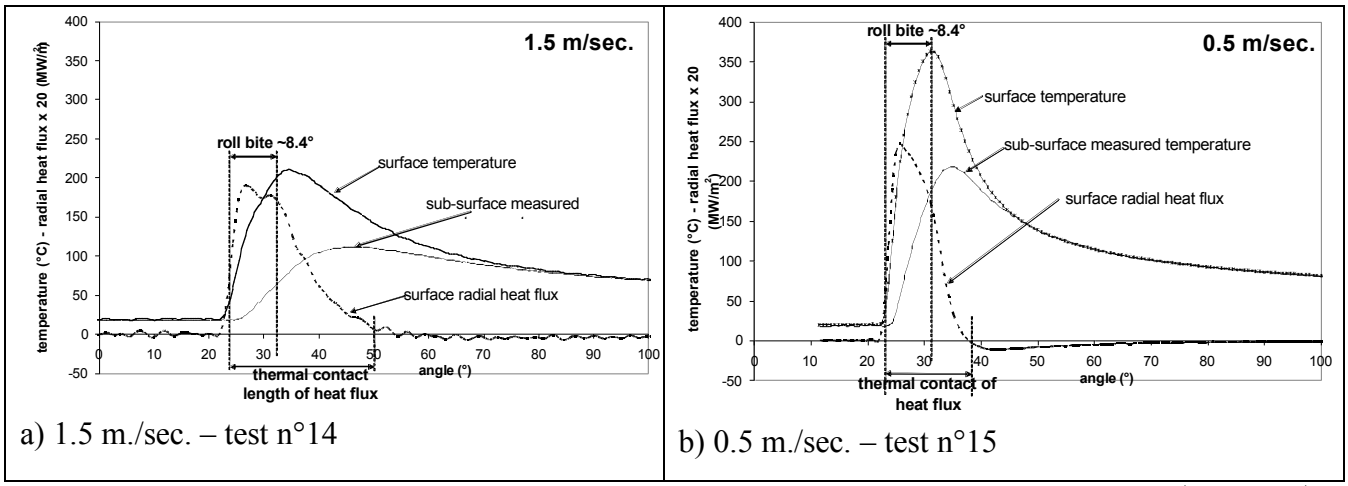

a) 1.5 m./sec. – test n°14

b) 0.5 m./sec. – test n°15

Fig.8: rolling speed influence on heat transfers, tests n°14 & 15, reduction = 10%, 1st pass, 1st revolution

It has been verified with the Hitchcock roll deformation model that these apparent post bite heat fluxes cannot be due to an error on the roll-strip contact length: the initial roll radius is practically unchanged with rolling load because the strip is very thick (60-40 mm). It has also been verified that these apparent post bite heat fluxes cannot be due to radiative heat transfers from strip to roll just after the direct contact: indeed radiation heat flux emitted by a strip at ~1000°C[2] is estimated at 0.14 MW/m^2, one order of magnitude lower than the post roll-bite heat fluxes visible on fig. 8-a.

Fig. 9 shows for 40% strip reduction the influence of rolling speed on the surface reconstruction: here, in contrast to 10% strip reduction, the heat flux length is in better agreement with the real contact length, especially for the lower speed (0.35 m/sec.). As a conclusion of the above analysis: at low speed (<0.5 m./sec.) and large contact lengths (reduction: 30 to 40%), the roll bite peak of heat flux reconstructed by inverse calculation is correct. At higher speeds (1.5 m./sec.) and smaller contact lengths (reduction : 10-20%), the reconstruction becomes incorrect (contact length overestimated), probably due to the fact that the thermocouple gives an average value in the section of the wire, which is more critical when speed increases (sharper gradients). Heat flux peak in the bite is under-estimated by the inverse calculation though its average value is correct.

[2] Radiation heat flux from a strip at 1000°C: $\varphi_{radiation} = \varepsilon.\sigma.\left[T_{strip}^{\ 4} - T_{environment}^{\ 4}\right]$. Numerical application: T_{strip} = 1000°C = 1273°K, $T_{environment}$ = 0, ε = 1, σ = 5.67.10-8 $W/m^2/K^4$ gives $\varphi_{radiation} = 0.14 MW/m^2$

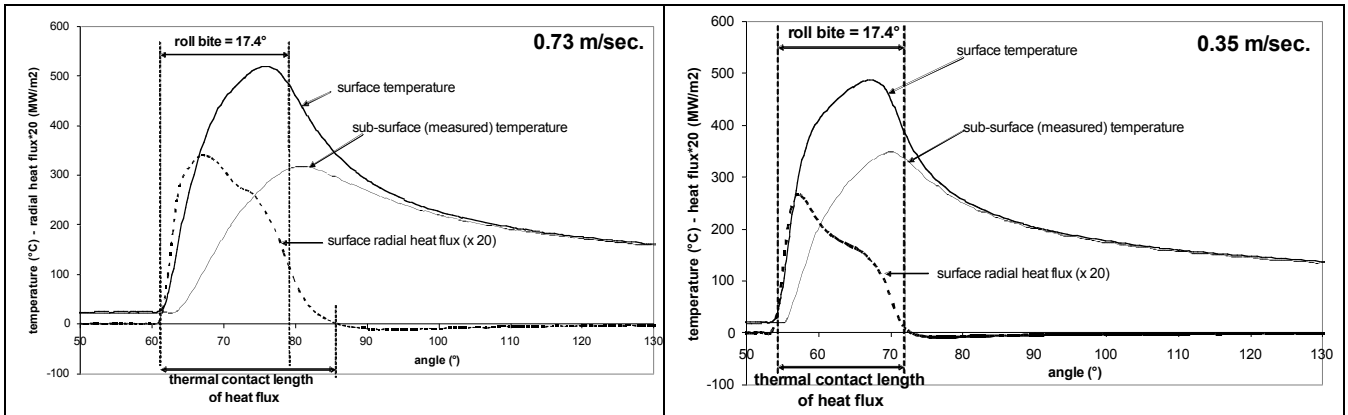

a) 0.73 m/sec. – test n°10 b) 0.35 m/sec. – test n°11

Fig.9: rolling speed influence on heat transfers – tests n°10&11 - strip reduction = 40% reduction.

Strip surface scale thickness influence on heat transfer

Fig.10 shows for two different initial scale thicknesses on strip surface the difference of heat flux in the roll bite during the first revolution of pass 1. In contrast to **[5]**, here the difference of scale thickness at strip surface before rolling was obtained with a difference of waiting time before rolling, while in **[5]**, this difference of scale thickness was obtained with a difference of heating furnace temperature. It seems for the present conditions (accordingly with **[5]**) that a higher scale thickness decrease heat transfers from strip to roll.

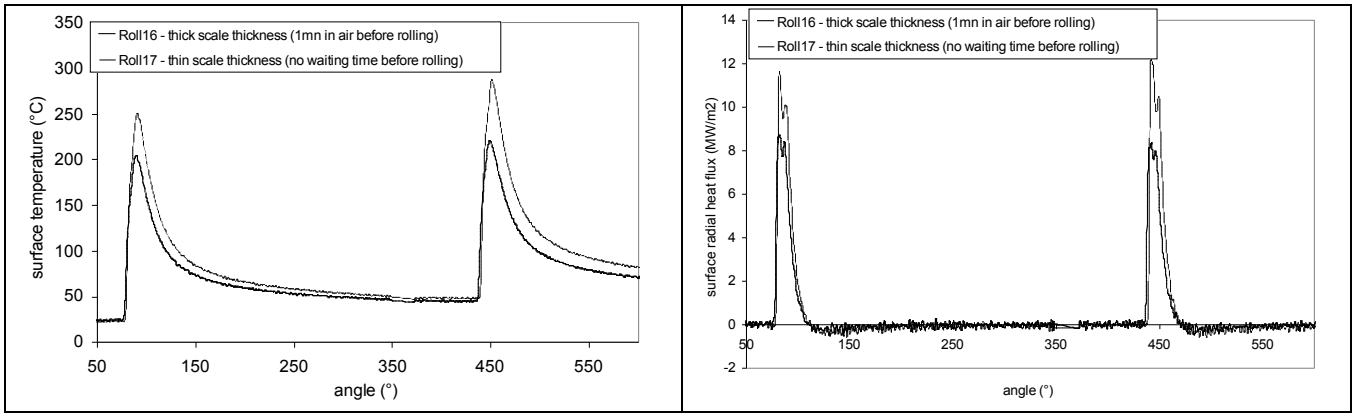

Fig.10: strip surface scale thickness influence on heat transfers – tests n°16&17 - reduction = 10%

Evaluation of roll bite Heat Transfer Coefficient $HTC_{roll\text{-}bite}$ by direct calculation *(model n°2)*

Model n°2 includes a strip thermal model and calculates heat transfers between roll and strip through $HTC_{roll\text{-}bite}$. Therefore, simulations presented in this section determine the equivalent thermal properties of the temperature sensor as well as the $HTC_{roll\text{-}bite}$ average value and its distribution along the bite using model n°2.

Sensor's solder material influence on sensor's thermal response

To characterize the thermal response of the temperature sensor composed with solder material (fig.4-b), two simulations have been performed with rolling conditions of test n°4 (table 1).

A first simulation with a $HTC_{roll\text{-}bite}$ uniform along the roll bite (same condition as **[5]**) and roll steel grade thermal properties are used (solder material of the sensor is not considered here). The 27,000 W/m/K $HTC_{roll\text{-}bite}$ value is adjusted on measured sub-surface temperature as already shown in **[5]**.

A second simulation was performed, still with a uniform $HTC_{roll\text{-}bite}$, but including the solder material properties of the temperature sensor (thermal diffusivity a = 4.2 mm^2/sec., thermal conductivity λ =17.3 W/m/K) which are slightly different from the roll steel grade thermal properties λ = 44 to 35 W/m/K and D = 11 to 6.5 mm^2/sec): the solder material is considered over a ~0.65 mm depth from the roll surface (fig.4-b) while for the rest steel material thermal property is considered. Here, $HTC_{roll\text{-}bite}$ is still considered uniform along the bite and its 23,000 W/m/K value is determined by adjusting sub-surface measured and sub-surface calculated temperatures.

Fig.11-a show that when considering solder material thermal properties in the simulation, the thermal response of the sensor is better predicted. However calculated surface heat flux with uniform $HTC_{roll\text{-}bite}$ has significant differences with the heat flux obtained by inverse analysis with model n°1 (fig.11-b).

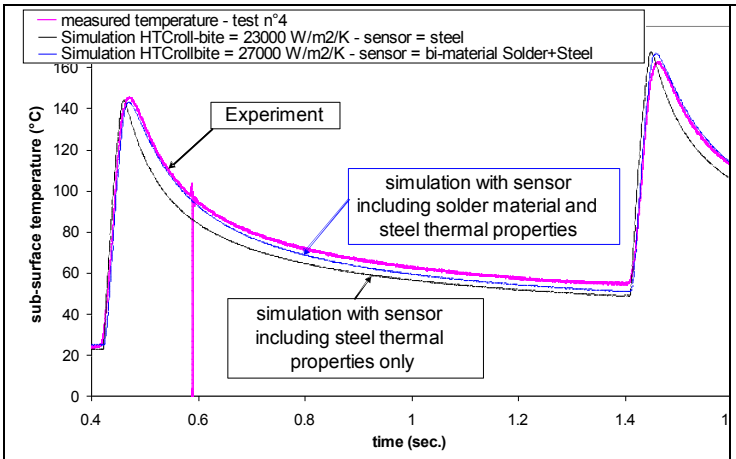

a) calculated and measured sub-surface temperatures with and without solder material

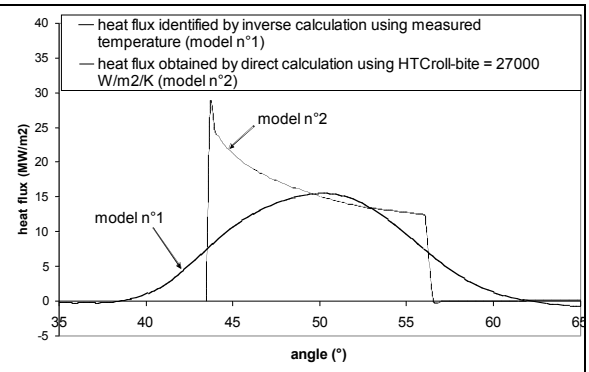

b) roll-surface heat flux with a uniform HTC roll-bite (model n°2) versus roll surface heat flux obtained by inverse calculation (model n°1)

Fig.11: a) influence of solder material on thermal response of the sensor (HTC roll-bite uniform): thermal properties of solder material over 0.65 mm from roll surface.
b) consequence of uniform HTC roll-bite on roll surface heat flux conditions: test n°4, 1st pass, two first revolutions

Evidence of a non uniform $HTC_{roll\text{-}bite}$ profile

To improve prediction of surface heat flux and surface temperature by direct simulation with model n°2, a non-uniform $HTC_{roll\text{-}bite}$ along the roll bite has been incorporated in the simulation (fig.12-a): the distribution has been defined in accordance with the classic rolling pressure distribution (fig.12-b) and was revealed a relatively good HTC distribution for roll bite heat flux profile prediction (fig.13-b).

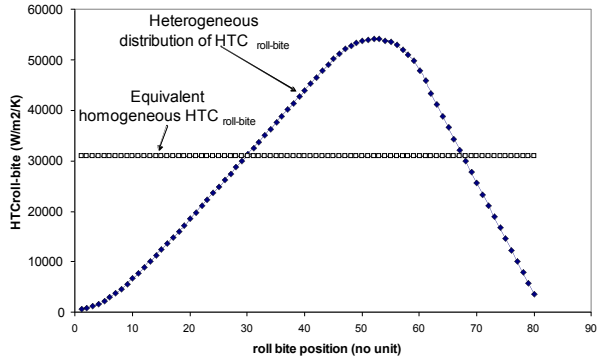

a) non uniform $HTC_{roll\text{-}bite}$ and equivalent homogeneous $HTC_{roll\text{-}bite}$

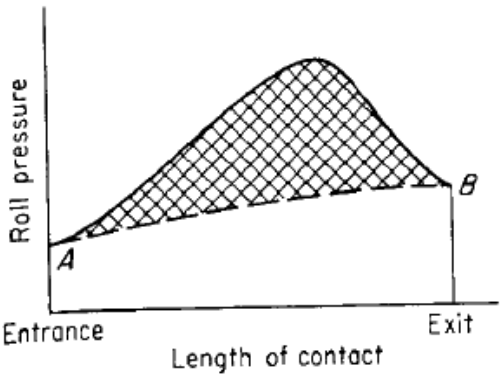

b) usual rolling pressure distribution

Fig.12: Correlation between HTC distribution along the roll bite for model n°2 and rolling pressure

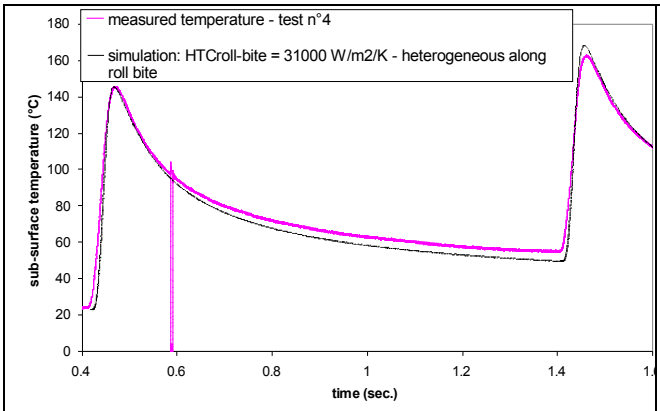

a) predicted/measured sub-surface temperature

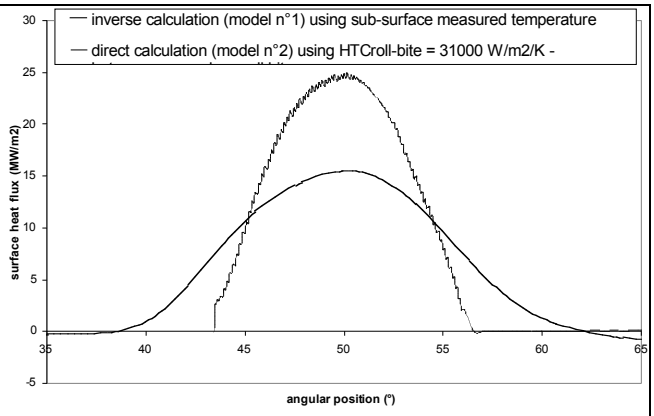

b) predicted surface heat flux with models n°1 and 2

Fig.13: calculated (model n°2) and measured sub-surface temperatures by considering thermal properties of solder material in the sensor – $HTC_{roll\text{-}bite}$ heterogeneous along the roll bite - test n°4, 1st pass, two first revolutions

More importantly, this non-uniform $HTC_{roll\text{-}bite}$ profile enables to obtain simultaneously a roll surface heat flux and surface temperature profiles in good agreement with the roll surface heat flux and temperature obtained by inverse calculation with model n°1 as shown in fig. 14.

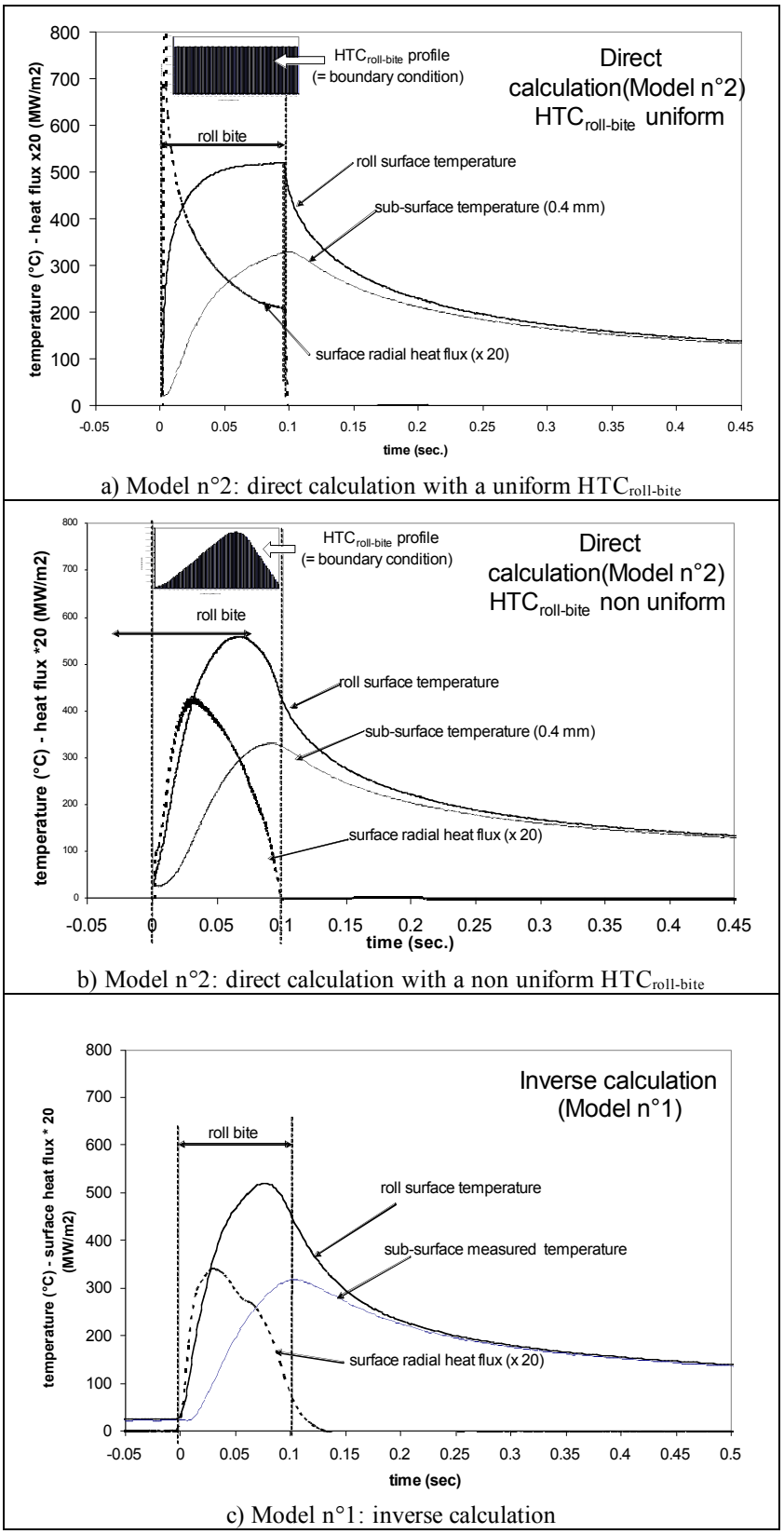

a) Model n°2: direct calculation with a uniform $HTC_{roll\text{-}bite}$

b) Model n°2: direct calculation with a non uniform $HTC_{roll\text{-}bite}$

c) Model n°1: inverse calculation

Fig.14: Comparison of direct calculation (model n°2) using uniform $HTC_{roll\text{-}bite}$ (a) and non uniform $HTC_{roll\text{-}bite}$ (b) with inverse calculation (model n°1) using measured sub-surface temperature
Simulation conditions : average $HTC_{roll\text{-}bite}$ = 50,000 W/m²/K, test n°10, 1st pass, first rotation

5. INFLUENCE OF $HTC_{roll\text{-}bite}$ DISTRIBUTION ON ROLL THERMAL FATIGUE DEGRADATION

The influence of the non-uniform $HTC_{roll\text{-}bite}$ on roll thermal fatigue has been evaluated using a thermal fatigue model from **[6]**. The industrial hot rolling conditions used for simulations correspond to the 4th stand of a 6-stands finishing hot strip mill (see section 3.): an average value of 90,000 $W/m^2/K$ for $HTC_{roll\text{-}bite}$ has been used and is considered to be a realistic value for the present rolling conditions where the maximum roll bite pressure is ~500 MPa. Figure 15-a show the non-uniform and uniform $HTC_{roll\text{-}bite}$ profile used in simulations.

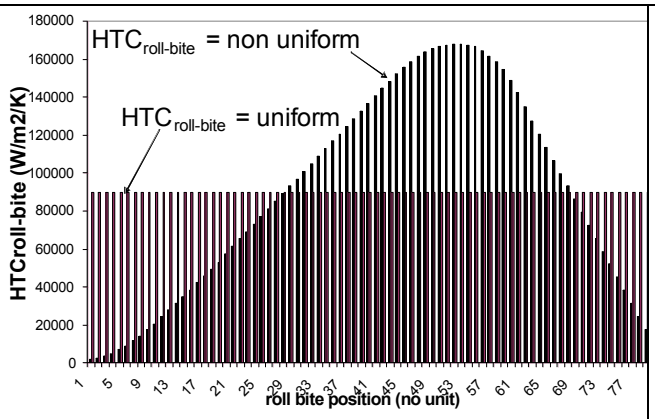

a) $HTC_{roll\text{-}bite}$ distribution: uniform /non uniform

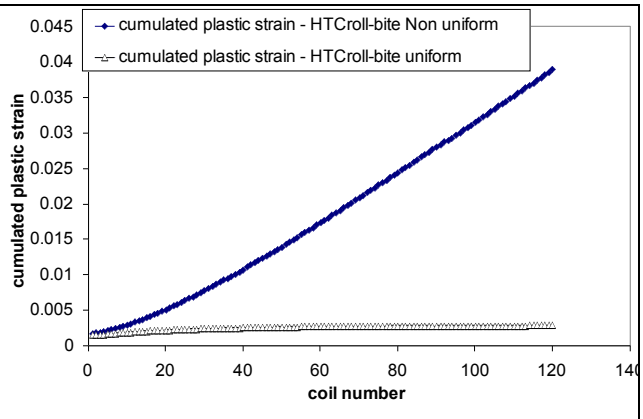

b) cumulated plastic strain with uniform and non uniform $HTC_{roll\text{-}bite}$

Fig.15: respective influence of uniform and non-uniform HTCroll-bite (a) on roll thermal fatigue degradation (b). (Industrial rolling conditions used are in §3)

Under the present conditions, the non-uniform $HTC_{roll\text{-}bite}$ increases cumulated plastic strain (fig.15-b) so increases roll thermal fatigue degradation in comparison to the uniform $HTC_{roll\text{-}bite}$ (same average value). For sake of simplicity, the $HTC_{roll\text{-}bite}$ profile is usually taken uniform in the rolling models, which is sufficient to optimize mill cooling capacity where only a knowledge of the average heat transfer within and from the roll is needed. The above results show however that to be realistic a roll thermal fatigue degradation model has to incorporate this non-uniformity of $HTC_{roll\ bite}$. It is also highlighted that the above simulation results (fig.15) do not have to be generalised, a systematic study of the correlation between $HTC_{roll\text{-}bite}$ distribution and roll thermal fatigue degradation should be done to be able to draw general conclusions.

6. CONCLUSIONS

Roll bite heat transfers in hot rolling have been identified with roll temperature sensors combined with simulations.

Simulation results: under industrial hot rolling conditions (rolling speed = 7 m./sec.), the temperature sensor with a high acquisition frequency (> 1000 Hz) predicts with a good accuracy (around 5% error) the roll bite peak of temperature. However, the peak of heat flux in the bite can be under-estimated (20% error) with noisy signal and thus the average roll bite heat flux is also valuable for industrial conditions. The above results are obtained from simulations and will be verified with a test on a full industrial mill of ArcelorMittal.
Pilot rolling test results: under pilot rolling conditions at low speed (<0.5 m./sec.) and large contact lengths (reduction: 30 to 40%), the roll bite heat flux peak reconstructed by inverse

calculation is correct. But at higher speeds (1.5 m./sec.) and smaller contact lengths (reduction : 10-20%), heat flux peak in the bite is under-estimated (contact length overestimated) by the inverse calculation though its average value is correct.

Furthermore, Heat Transfer Coefficient $HTC_{roll\text{-}bite}$ is not uniform along the roll bite but is proportional to the local rolling pressure. Moreover, roll thermal fatigue simulations have shown that this non-uniform $HTC_{roll\text{-}bite}$ can affect the roll fatigue degradation significantly in the rolling condition used in this paper and thus it has been incorporated in the model to improve its accuracy.

References

[1] P.Kotrbacek, M. Raudensky, J. Horsky, M. Pohanka, Experimental study of heat transfer and heat flux by inverse analysis during steel strip rolling, Revue de metalurgie 103 (2006) 333-341.

[2] D. Weisz-Patrault, A. Ehrlacher, N. Legrand, N. Labbe, J.Horsky, T.Luks. Experimental study of interfacial heat flux and surface temperature by inverse thermal analysis with thermocouple (fully embedded) during hot steel strip rolling. Advanced Materials Research. 452-453 (2012) 959-963

[3] D. Weisz-Patrault, A. Ehrlacher, N. Legrand, Evaluation of temperature field and heat flux by inverse analysis during steel strip rolling. International Journal of Heat and Mass Transfer 55 (2012) 629-641

[4] User's manual of Cylescale, roll and strip temperature evolution model – Arcelormittal internal report. M. Picard (2009)

[5] Analysis of roll bite heat transfers in hot steel strip rolling through roll temperature sensors and heat transfer models. N. Legrand, N. Labbe, D. Weisz-Patrault, A. Ehrlacher, J.Horsky, T.Luks. Key Engineering Materials 504-506 (2012) 1043-1048

[6] A tool to evaluate work roll damage due to thermal fatigue in the hot strip mill. E. Mathey, C. Cera, C. Brito-Ferreira, M. Mohammadi-Terhani, M. Picard, AIST Conference, May 5-8, 2008, Pittsburgh, Pa USA

Y. Loup, A. Ait Bengrir T. Lavalard, J.N. Fouligny and E. Mathey from ArcelorMittal Maizières Research are acknowledged for preparation of rolling tests and help in simulations with the roll thermal fatigue model.